Published by
NIGERIAN SOCIETY OF PHYSICAL SCIENCES
Available online @ https://journal.nsps.org.ng/index.php/jnsps

J. Nig. Soc. Phys. Sci. 7 (2025) 2503

Journal of the Nigerian Society of Physical Sciences

Comprehensive study of photon and proton interactions to interpret the radiation parameters of boron derivative drugs for chemoradiotherapy

A. M. Olaosun[a,*], C. A. Aborisade[a], D. E. Shian[b], O. O. Oloyede[c], P. T. Osuolale[d]

[a]*Department of Physics and Science Laboratory Technology, Abiola Ajimobi Technical University, P.M.B. 5015, Ibadan, Oyo State, Nigeria*
[b]*The Institute of Biomedical and Oral Research, Faculty of Dental Medicine, The Hebrew University of Jerusalem, P.O.B. 12272, Ein Kerem, Jerusalem, ISRAEL 91120*
[c]*Department of Pure and Applied physics LAUTECH, Ogbomoso, P.M.B 4000, Ogbomoso, Oyo-Sate, Nigeria*
[d]*Department of Information Systems and Technology, Kings University, Odeomu, Osun-State, Nigeria*

Abstract

For chemoradiotherapy applications, this work investigated the photon and proton interaction parameters in five boron-based medications: sodium borocaptate, bortezomib, delanzomib, boronophenylalanine, and boric acid. Photon interaction parameters such as the mass attenuation coefficient, effective atomic number, effective electron density, and buildup variables were computed. The effective atomic number and stopping power for proton interactions were determined by calculating mass stopping cross-sections, which allowed for the computation of the effective electron density. Below 0.1 MeV, the highest value of mass attenuation coefficient and effective atomic number was found for sodium borocaptate and boric acid, respectively. Among the medications, boric acid had the highest effective atomic number for proton interactions. Both photon and proton interactions showed a direct correlation between electron density and effective atomic number. In the areas where medication variations were most noticeable, bortezomib showed the highest values for buildup factors. The mass stopping power and mass stopping cross-section peaked at about 0.1 MeV, with delanzomib and bortezomib exhibiting especially high values at lower energies. This study is expected to provide understanding about the radiation interaction parameters of the investigated boron derivative drugs, which will in turn guide their administration and effectiveness in enhancing photon and proton radiations for chemoradiotherapy purposes.

DOI:10.46481/jnsps.2025.2503

Keywords: Boron derivative drugs, Chemoradiotherapy, Radiation parameter, Effective atomic number

Article History :
Received: 13 November 2024
Received in revised form: 12 March 2025
Accepted for publication: 28 March 2025
Published: 16 April 2025

Communicated by: C. A. Onate

1. Introduction

In medicine, ionizing radiation performs a major role in diagnosing (diagnostic radiology) and treating (therapeutic radiology) illnesses [1, 2], as it has the ability to acquire images of various sections of the human body and also to destroy tumors or cells, respectively [3]. One of the leading aspects of the applications of radiotherapy is in the management of cancer. In cancer management, approximately 50 percent of all newly diagnosed cancer cases require radiotherapy at one point or another [4, 5]. As such, in radiotherapy, ionizing radiation

*Corresponding author Tel. No: +234-806-712-5750.
Email address: abayomi.olaosun@tech-u.edu.ng (A. M. Olaosun)

kills or controls the growth of cancer cells [6]. Aside from radiotherapy, chemotherapy, which involves the use of drugs, is another important method in managing cancer, especially for cancers complicated with metastasis [7]. However, the inability to completely eradicate cancer stem cells is likely one of the main factors contributing to the poor efficacy of chemotherapy in treating some cancers [7]. As such, chemoradiation, which involves the combination of chemotherapy and radiotherapy, is important in order to enhance treatment outcomes during cancer management. Common chemoradiation includes concurrent chemoradiation (chemotherapy and radiation are given concurrently); sequential chemoradiation (chemotherapy is given after radiotherapy); and adjuvant chemoradiation (chemotherapy and radiation are given after surgery).

In terms of radiation response, the interaction of radiation with human tissues, biomolecules, and drugs, are characterized by energy, type of radiation, and absorbed dose. Therefore, interaction of radiation with chemotherapy drugs are important in chemoradiation [8]. As a result of this, several studies have investigated radiation interaction parameters for some chemotherapy drugs [8–17]. For photons interaction, radiation parameters investigated for different chemotherapy drugs include the effective atomic number (Z_{eff},), effective electron density, mass attenuation coefficient (μ/ρ), exposure buildup factor (EBF), and energy absorption buildup factor (EABF) [12–14]. For proton interaction, the investigated parameters include the Z_{eff}, N_{eff}, and mass stopping power ($S(E)/\rho$) [8, 9]. In the context of radiation interaction, Z_{eff} is an important content that describes the atomic number of a composite material at different energies [8, 17]. Furthermore, in radiation fields, Z_{eff} is important in predicting radiation absorption, calculating radiation dose, determining radiation attenuation, and modeling radiation transportation [10, 18]. On the other hand, N_{eff} is the number of electrons per unit mass for a multi-elemental material. This parameter is equally important in predicting radiation absorption, attenuation, and dose calculation [10, 16]. The μ/ρ of a material is the ratio of its linear attenuation coefficient (μ) to its density (ρ). By implication, it is a measure of the attenuation of radiation as it traverses material as normalized by the material's density, thus representing the probability of radiation interactions per unit mass of the material. In various fields like medical physics, μ/ρ is a basic photon radiation parameter in evaluating other radiation interaction parameters such as the deposition of energy, dosimetric behavior, N_{eff}, and Z_{eff}, among others [9, 19]. When a photon interacts with material, new photons can emerge due to multiple scattering. Such multiple scattering is quantified by the buildup factor. The buildup factor depends on the atomic number of the absorbing material, the energy of the photon beam, the penetration depth, and the form of the radiation source and medium. EBF and EABF are the two types of buildup factors. The EBF and EABF are the buildup factors when the quantity of interest is the energy deposited in air and the absorbing material, respectively [20–22]. In charged particle radiations (electrons, protons, and other heavy ions), the extent to which charged particles penetrate a given material is quantified by $S(E)/\rho$. It is the ratio of the stopping power of a charged particle to the material density. This parameter, which is important in determining the range of charged particles in a material, depends on the atomic number and density of the interacting material as well as the energy of the charged particle [23]. On the other hand, the mass stopping cross-section (S_c) depends on the atomic number of the interacting medium and the mass and velocity of the charged particle. The Z_{eff} of charged particle radiation, which is a decisive parameter in particle therapy and ion implantation, can be determined by mass stopping cross-section [24].

Boron derivatives have shown their potential as chemotherapy drugs in cancer management due to their antitumor properties [25–28]. Some of these boron containing drugs include bortezomib [29], talabostat [30–32], boric acid [33, 34], delanzomib [35, 36], sodium borocaptate, and boronophenylalanine [37]. Moving forward, studies have used boron derivatives concurrently with external beam radiation in treating cancer [29, 38]. The current practice of clinical radiotherapy mostly utilizes photon beams. This is because photon radiation has shown a well proven efficacy, abundance of high-intensity sources, simplicity of precise beam location and dose field calculation, and lower treatment cost. On the contrary, protons and heavier ions are used to treat less than 1% of patients worldwide. This is most likely to be as a result of sophisticated equipment, high treatment costs, and the paucity of data supporting its superior effectiveness over less expensive photon-based treatments. However, proton and ion therapy have progressed rapidly in the last several decades, with novel treatment methods and several specialized radiation facilities being constructed worldwide [39–42]. Furthermore, in practice, proton beam therapy is gaining popularity as it offers a more conformal dose distribution to the tumor, thus reducing unintending radiation to the normal tissue, a challenge that is common to conventional photon therapy. This is because most of its energy is deposited within a point known as the Bragg peak [40]. Moreover, aside from photons, literature has revealed that boron compounds also enhance proton beam therapy using the Proton Boron Capture Therapy (PBCT) technique [42–44]. Despite the undeniable potential and abilities showcased by boron derivatives in enhancing photon and proton therapies, it is, however noticed that there is no such study in the literature that has investigated the photon and proton interaction parameters for these derivatives. Therefore, this study aims to investigate the photon and proton interaction parameters for boric acid (BA), boronophenylalanine (BP), bortezomib (BZ), delanzomib (DZ), and sodium borocaptate (SB) drugs.

2. Materials and methods

In literature, several studies have utilized an online window package, WinXCom [45], for computing radiation interaction parameters for different materials. However, its usefulness is limited because it can only compute radiation parameters for photon radiation. Also, the PSTAR code that has been widely utilized in computing proton radiation parameters for different materials [46] is also limited as it can only directly account for 26 elements and 48 preset compounds/mixtures [18]. Therefore, in this study, PAGEX computer software [24] was utilized

in order to calculate the investigated photon and proton interaction parameters for the selected boron derivative drugs (BA, BP, BZ, DZ, and SB) that are presented in Table 1. In brief, PAGEX is a cross-platform software designed to quickly calculate both photon (X-ray and gamma-ray) and charged particle interaction parameters. These include mass attenuation coefficients, partial/total photon interaction cross-sections, electron density, effective atomic number, and buildup factors, as well as mass-energy absorption coefficient over a wide energy range. It is easy to use and has demonstrated good agreement when cross-checked against WinXCom and PSTAR, among other popular programs and datasets [24]. The theoretical approach to the use of PAGEX software in computing the μ/ρ, Z_{eff}, N_{eff}, EBF, EABF, S(E)/ρ, and S_c are further given.

2.1. Mass attenuation coefficient (μ/ρ)

For a multielement material, its μ/ρ is expressed using mixture rule [10],

$$\mu/\rho\ (cm^2/g) = \sum_i w_i \left(\frac{\mu}{\rho}\right)_i, \tag{1}$$

where w_i and $\left(\frac{\mu}{\rho}\right)_i$ are the weight fraction and mass attenuation coefficient of the individual elements present in the material. The μ/ρ of the investigated boron derivative drugs have been computed using the online software package, WinXCom [45].

2.2. Effective atomic number (Z_{eff}) and effective electron density (N_{eff})

The Z_{eff} for photon radiation is expressed as:

$$Z_{eff} = \frac{\sigma_a}{\sigma_e}, \tag{2}$$

where $\sigma_a \left(= \frac{\sum_i f_i A_i (\mu/\rho)_i}{N_A}\right)$ and $\sigma_e \left(= \frac{\sum_i \frac{f_i A_i (\mu/\rho)_i}{Z_i}}{N_A}\right)$ in the unit of b/atom and b/electron are the average effective cross-section per atom and average effective cross-section per electron, respectively for which N_A is the Avogadro's constant and f_i, A_i, Z_i are the number fraction, atomic weight, and atomic number of the ith element, respectively. For proton radiation Z_{eff} of multielement material is expressed as:

$$Z_{eff} = \frac{Z_1 (\log S_{c2} - \log S_c) + Z_2 (\log S_c - \log S_{c1})}{\log S_{c2} - \log S_{c1}}, \tag{3}$$

where S_{c1} and S_{c2} are the mass stopping cross-section, at a given proton energy, corresponding respectively to elements with atomic numbers Z_1 and Z_2 within which the mass stopping cross-section (S_c) of the multielement material lies.

For photon and proton radiations, the Z_{eff} obtained is related to the N_{eff} and expressed as:

$$N_{eff} = N_A \frac{Z_{eff}}{< A >}, \tag{4}$$

where N_A is the Avogadro's constant, and $< A >$ is the average atomic mass of multielement material.

2.3. Exposure Buildup Factor (EBF) and Energy Absorption Buildup Factor (EABF)

The buildup factor (BF) for both EBF and EABF is computed based on mathematical expression given as:

$$BF\,(E, x) = \begin{cases} 1 + \frac{b-1}{k-1}\,(k^x - 1), & for\ k \neq 1 \\ 1 + (b-1)\,x, & for\ k = 1 \end{cases}, \tag{5}$$

where E is the incident photon energy, x is the depth of penetration in the unit of mean free path (MFP), $k\left(= cx^a + d\frac{tanh(x/X_k - 2) - \tanh(-2)}{1 - \tanh(-2)}\ for\ x \leq 40\ mfp\right)$ is the multiplication factor, and X_k, d, c, b, and a are the G-P fitting parameters.

2.4. Mass stopping power (S(E)/ρ) and mass stopping cross-section (S_c)

S(E)/ρ and S_c are peculiar to charged particle radiation, in this study proton radiation. For a multielement material, S(E)/ρ is expressed as:

$$\mathrm{S(E)/\rho}\ \left(MeV\ cm^2/g\right) = \sum_i w_i (S(E)/\rho)_i, \tag{6}$$

where $(S(E)/\rho)_i$ and w_i are the mass stopping power and weight fraction of ith element present in the multielement material. The S_c is related to S(E)/ρ and is expressed as:

$$S_c\ \left(MeV\ cm^2/atom\right) = \frac{S(E)/\rho}{N_A \sum_i (w_i/A_i)}, \tag{7}$$

where A_i is the atomic number of the ith element present in the multielement material and $S(E)/\rho$, N_A, and w_i have their usual meaning.

3. Results and discussion

3.1. Mass attenuation coefficient (μ/ρ)

The μ/ρ, which is the basic parameter for finding other radiation parameters for photon interaction, has been calculated. This parameter is essential as it is used in explaining different scattering and absorption events associated with the photon as it traverses materials. Figure 1 presents the variation of μ/ρ of the selected boron derivative drugs in this study. In photon interaction with matter, the photoelectric effect, Compton scattering, and pair production are the probable modes of interaction that take place at lower (E ≤ 0.1 MeV), intermediate (0.1 ≤ E ≤ 1 MeV), and higher (E ≥ 1 MeV) energy regions, respectively. During the photoelectric effect, a photon is completely absorbed. As such, as the energy increases, μ/ρ decreases. This trend was absorbed in the lower energy region (E ≤ 0.1 MeV) presented in Figure 1.

The μ/ρ of the boron derivative drugs decreases as the energy of the photon energy increases up to 0.1 MeV. Furthermore, in this region, it was observed that the μ/ρ depends on the chemical compositions of the boron derivative drugs considered. As such, variation was observed in the values of μ/ρ of the selected boron derivative drugs. The highest and lowest values of μ/ρ were observed for SB and BZ, respectively. Considering the elemental compositions (Table 1), SB consists of

Table 1. Chemical formula and elemental composition of the selected drugs.

Drug	Chemical formula	Molecular weight(g/mol)	Composition (%)						
			H	B	C	N	O	Na	S
BA	BH_3O_3	61.84	4.9	17.48	-	-	77.62	-	-
BP	$C_9H_{12}BNO_4$	209.03	5.8	5.17	51.73	6.7	30.6	-	-
BZ	$C_{19}H_{25}BN_4O_4$	384.29	6.57	2.81	59.38	14.59	16.65	-	-
DZ	$C_{21}H_{28}BN_3O_5$	413.33	6.85	2.62	61.05	10.17	19.31	-	-
SB	$B_{12}H_{12}Na_2S$	219.89	5.51	59.04	-	-	-	20.92	14.53

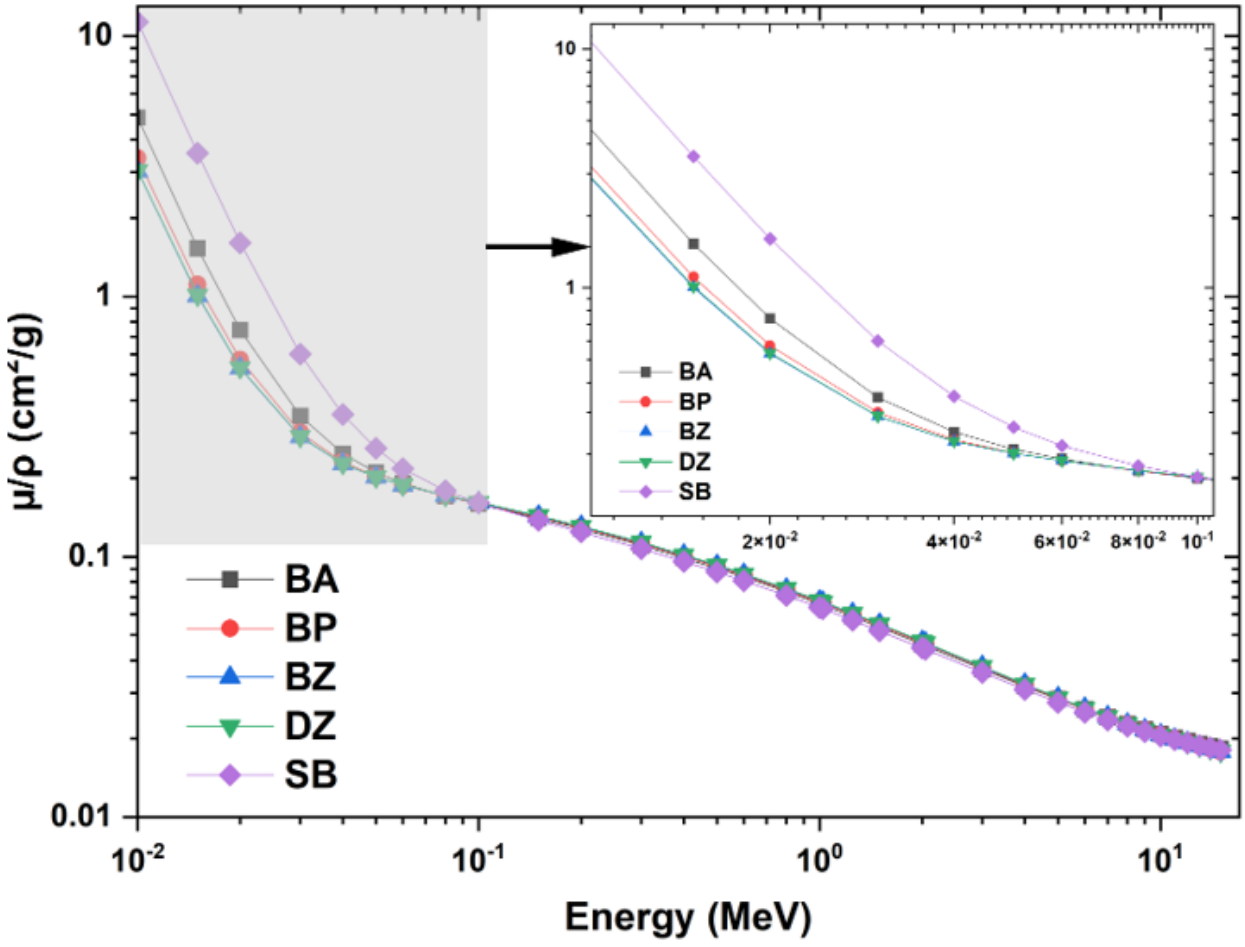

Figure 1. Variation of mass attenuation coefficient (μ/ρ) of drugs with energy for photon interaction.

heavier elements (Na and S) compared to other drugs. Therefore, it attenuates more photons relatively to others due to the presence of these heavier elements. For the remaining drugs, BA, BP, DZ, and BZ, the heaviest element present in them is oxygen. The variation of μ/ρ among them can be explained in terms of the percentage weight of oxygen present in them. The percentage weights of oxygen present in BA, BP, DZ, and BZ are 77.62, 30.6, 19.31, and 16.65, respectively (Table 1). Thus, among these other four drugs, BA has the highest value of μ/ρ. This is followed by BP, DZ, and BZ, respectively. Overall, the order of μ/ρ observed among the boron derivative drugs was SB > BA > BP > DZ > BZ. In this study, the investigated drugs are boron derivatives. Therefore, in terms of the percentage weight of boron present in each of the drugs (Table 1), it follows that at the low energy region, the μ/ρ increases as the percentage weight of boron present in the drugs increases. Therefore, in the lower energy region, SB and BZ, which, respectively, have the maximum and least value of boron concentration, will have the maximum and least enhancement factor for photon interaction, respectively.

At the higher energy region (E ≥ 0.1 MeV), the μ/ρ slightly decreases as the energy increases. Furthermore, there is no observable difference in the value of μ/ρ of the boron derivative drugs. This is because of the domination of Compton scattering, which occurs with the transitions to higher energies. As such, the chemical compositions of the drugs lose their relevance in the likelihood of photon interaction [9, 47]. In photon therapy, X-ray and gamma-ray are the two radiations that are

Table 2. Mass attenuation coefficient (μ/ρ) for photon interaction at therapeutic energy range 0.1–15 MeV.

Energy (MeV)	μ/ρ (cm^2/g)				
	BA	BP	BZ	DZ	SB
0.100	0.159	0.160	0.161	0.162	0.161
0.150	0.140	0.142	0.143	0.144	0.138
0.200	0.128	0.130	0.131	0.131	0.124
0.300	0.111	0.112	0.113	0.114	0.107
0.400	0.099	0.101	0.101	0.102	0.096
0.500	0.090	0.092	0.093	0.093	0.087
0.600	0.084	0.085	0.086	0.086	0.081
0.800	0.073	0.075	0.075	0.075	0.071
1.000	0.066	0.067	0.068	0.068	0.064
1.022	0.065	0.066	0.067	0.067	0.063
1.250	0.059	0.060	0.060	0.061	0.057
1.500	0.054	0.055	0.055	0.055	0.052
2.000	0.046	0.047	0.047	0.047	0.045
2.044	0.046	0.046	0.047	0.047	0.044
3.000	0.037	0.038	0.038	0.038	0.036
4.000	0.032	0.032	0.032	0.032	0.031
5.000	0.028	0.029	0.029	0.029	0.028
6.000	0.026	0.026	0.026	0.026	0.025
7.000	0.024	0.024	0.024	0.024	0.024
8.000	0.023	0.023	0.023	0.023	0.022
9.000	0.022	0.022	0.022	0.022	0.021
10.000	0.021	0.021	0.021	0.021	0.020
11.000	0.020	0.020	0.020	0.020	0.020
12.000	0.020	0.019	0.019	0.019	0.019
13.000	0.019	0.019	0.019	0.019	0.019
14.000	0.019	0.018	0.018	0.018	0.018
15.000	0.018	0.018	0.018	0.018	0.018

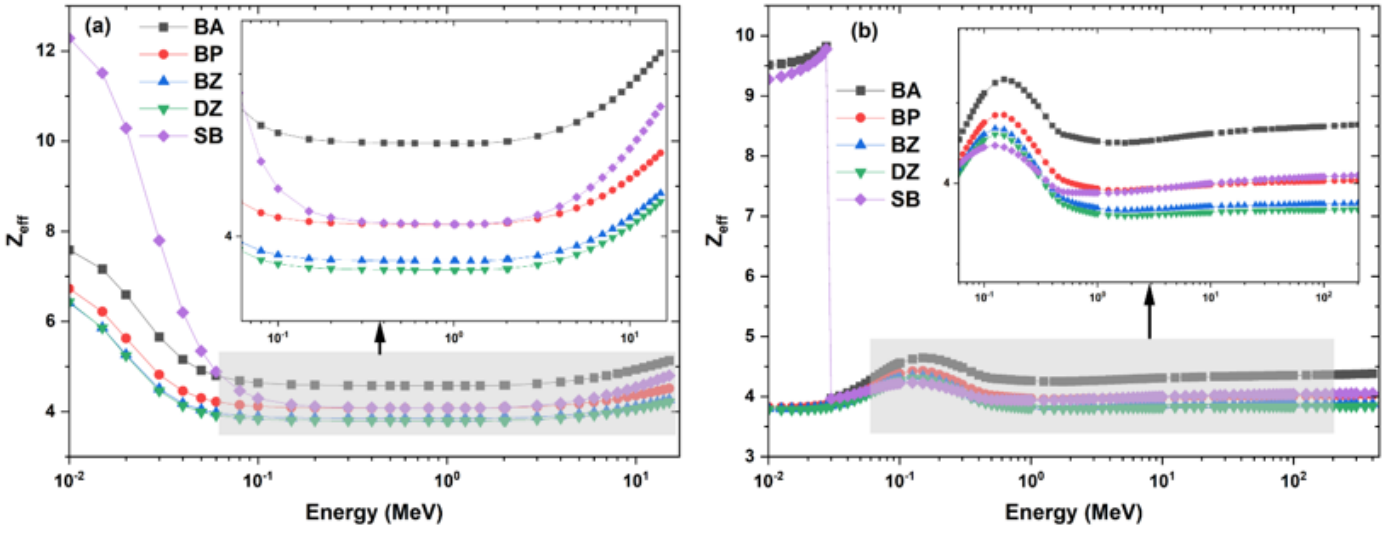

Figure 2. Variation of effective atomic number (Z_{eff}) of drugs with energy for (a) photon and (b) proton interactions.

employed. For X-ray therapy, orthovoltage (0.1–0.5 MeV) and megavoltage (1–25 MeV) are applicable in treating superficial and deep-seated tumors [48–51]. However, for megavoltage beams, energy above 15 MeV is unusual in clinical practices. For gamma ray, the energy of gamma ray emitted from commonly used radionuclides in radiotherapy has a range of about 0.3–1.5 MeV [52]. Combining these energies in a range of 0.1–15 MeV, the μ/ρ of the drugs are provided in Table 2. The result obtained in this therapeutic energy range showed that the differences in the elemental composition of each of the drugs have

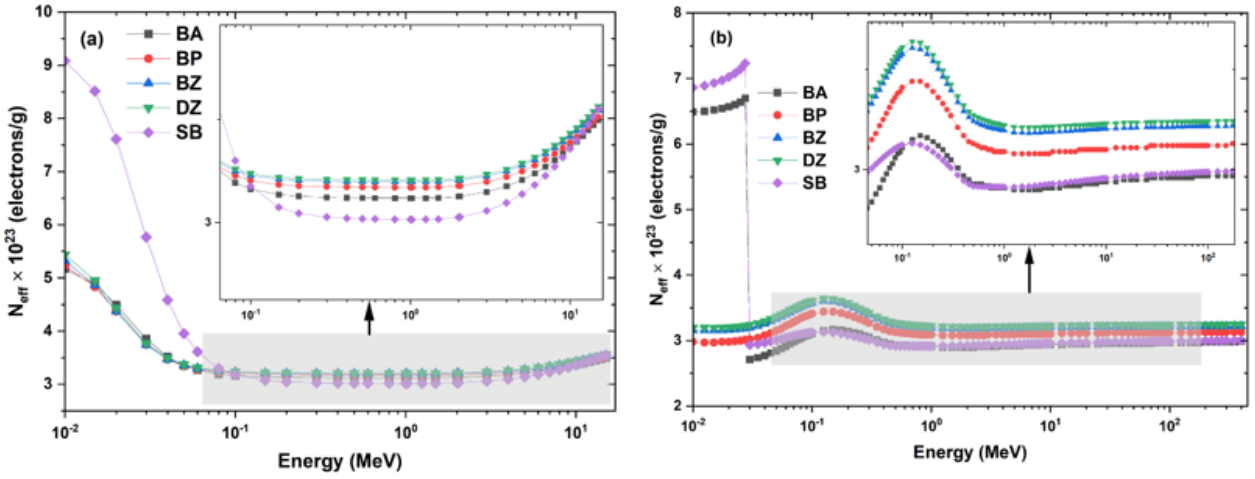

Figure 3. Variation of effective electron density (N_{eff}) of drugs with energy for (a) photon and (b) proton interactions .

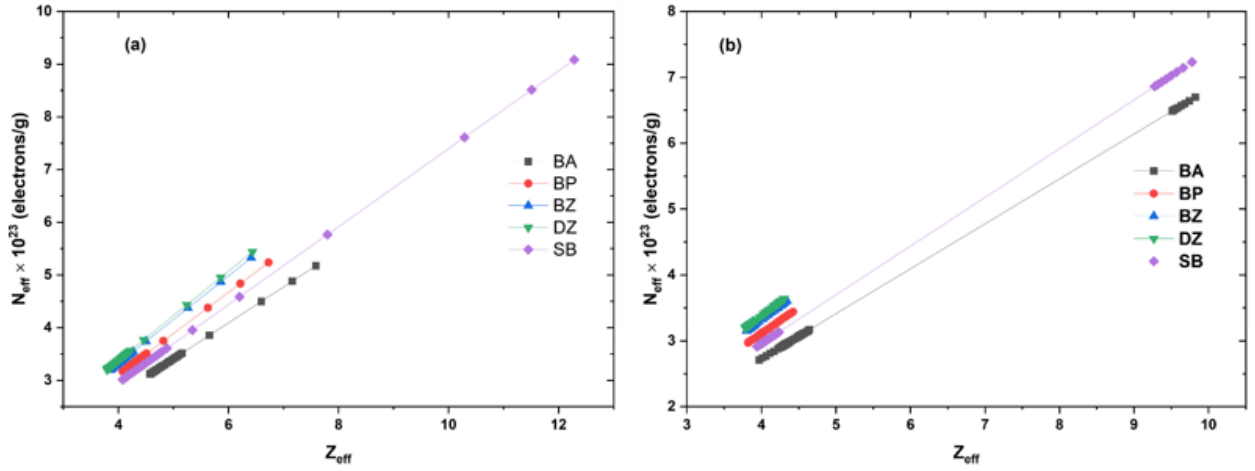

Figure 4. Variation of effective electron density (N_{eff}) of drugs with their respective effective atomic number (Z_{eff}) for (a) photon and (b) proton interactions.

Table 3. Mass stopping power (S(E)/ρ) for proton interaction at therapeutic energy range 70–250 MeV.

Energy (MeV)	S(E)/ρ (MeV cm^2/g)				
	BA	BP	BZ	DZ	SB
70	8.939	9.130	9.245	9.272	8.762
75	8.476	8.656	8.765	8.791	8.308
80	8.067	8.237	8.340	8.364	7.907
85	7.703	7.864	7.962	7.986	7.550
90	7.377	7.531	7.625	7.647	7.231
95	7.083	7.231	7.320	7.342	6.943
100	6.817	6.959	7.044	7.065	6.682
125	5.791	5.909	5.982	5.999	5.677
150	5.093	5.195	5.257	5.273	4.991
175	4.586	4.677	4.733	4.747	4.494
200	4.202	4.283	4.334	4.347	4.117
225	3.900	3.975	4.022	4.034	3.820
250	3.657	3.726	3.770	3.781	3.582

little or no effect on the difference in the μ/ρ obtained among the drugs. Therefore, in the therapeutic energy range, the investigated boron derivative drugs will enhance photon radiation with a similar factor.

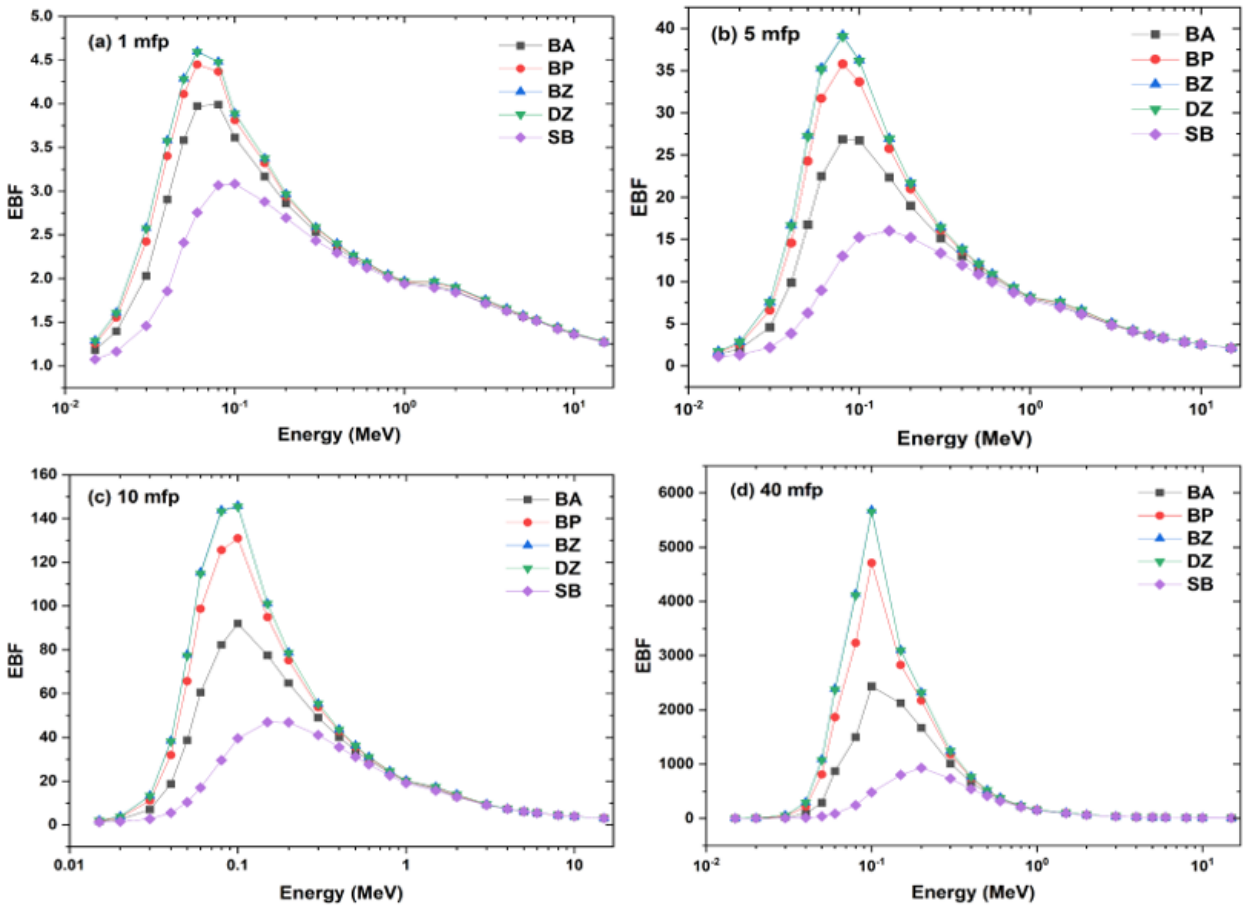

Figure 5. Variation of exposure buildup factor (EBF) of drugs with energy at (a) 1, (b) 5 (c) 10, (d) 40 MFPs penetration depths for photon interaction.

3.2. *Effective atomic number (Z_{eff}) and effective electron density (N_{eff})*

In understanding the behavior of the interaction of radiation with matter, Z_{eff} is an important parameter that expresses the physical behavior in terms of the atomic number of any composite material with a variety of atoms. For complex mediums, this parameter depends on energy [10]. Since the boron derivative drugs investigated in this study consist of different elements (Table 1), it is thus important to investigate their Z_{eff}. The variations of Z_{eff} of the selected boron derivative drugs with energy are presented in Figures 2a and 2b for photon and proton interactions, respectively. For photon interaction, Figure 2a, the Z_{eff} of all the drugs experienced similar variations across the range of energy considered (0.01–15 MeV). Going by the increase in energy, the Z_{eff} decreases sharply from 0.01 to about 0.1 MeV. At this region, the observable order is SB > BA > BP > DZ > BZ. At other energies (E ≥ 0.1 MeV), the Z_{eff} of BA and DZ, among other drugs, shows maximum and minimum value, respectively. These other energies are further classified into the Compton scattering region (0.1 ≤ E ≤ 1 MeV), for which the Z_{eff} for each of the drugs remains almost constant as the energy increases, and the pair production region (E ≥ 1 MeV), for which the Z_{eff} slightly increases as the photon energy increases. This slight increase is caused by the initiations, but not prominent, of pair production at energy of about 1.022 MeV which later become little prominent at energy greater than 2 MeV. For proton interaction, Figure 2b, except BA and SB, Z_{eff} were found to be smaller at the lower energy region. SB has elements with a higher atomic number (Na and S) when compared to other drugs, while BA has the highest percentage weight of oxygen among the remaining drugs. This is likely the reason why both drugs exhibit a jump in the value of Z_{eff} at lower energy. The value of Z_{eff} further slightly increases and later attained its highest value around 0.1 MeV. Away from 0.1 MeV, the value of Z_{eff} further decreases as the energy increases up to about 1 MeV. At the higher energy region (E > 1 MeV), the Z_{eff} slightly increases as the energy increases. On average, maximum and minimum values of Z_{eff} were observed for BA and DZ, respectively, among the drugs. Figures 3a and 3b present the variation of N_{eff} of the drugs with energy for photon and proton interactions, respectively. For both interactions, it is observed that the N_{eff} for each of the drugs follows similar energy habituation as their respective Z_{eff}. This is because of the direct relation that exists between Z_{eff} and N_{eff} (Eq. 4). Similar results have been reported in previous studies [8, 10, 18, 53]. This direct relation between these two parameters is further depicted in Figures 4a and 4b for photon and proton interactions, respectively.

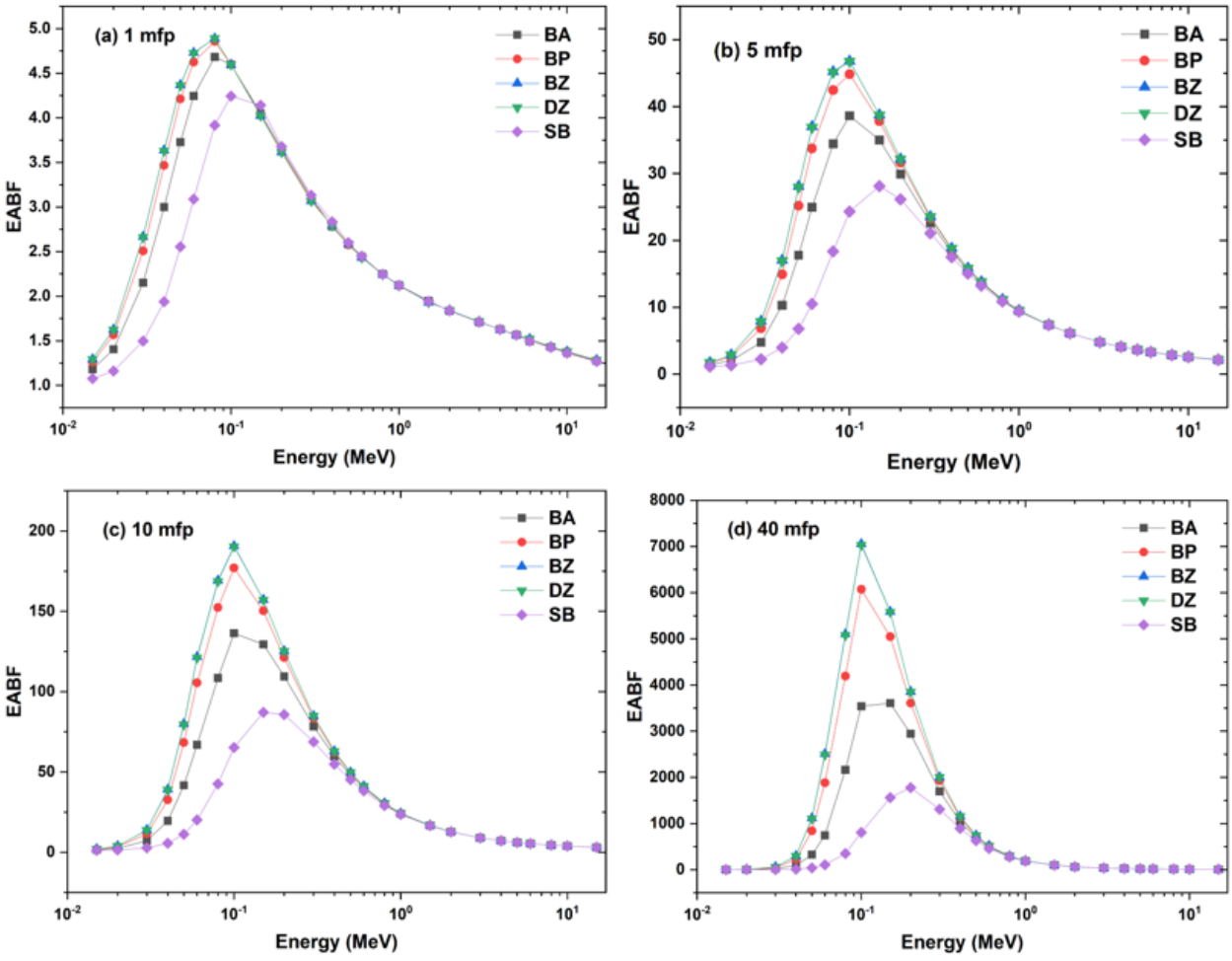

Figure 6. Variation of energy absorption buildup factor of drugs with energy at (a) 1, (b) 5, (c) 10, and (d) 40 MFPs penetration depths for photon interaction.

3.3. *Exposure Buildup Factor (EBF) and Energy Absorption Buildup Factor (EABF)*

In this study, buildup factors (EBF and EABF) of the selected boron derivative drugs have been investigated. Figures 5a – 5d and 6a – 6d depict the variation of EBF and EABF of the drugs with photon energies in the range of 0.015–15 MeV at 1, 5, 10, and 40 penetration depths (MFPs), respectively. In radiation fields, EBF and EABF are important parameters in calculating radiation dose. These two parameters, including scattering, are important to have a deep understanding of the absorption effect in broad-beam transmission work [47]. From the result obtained, EBF and EABF of each of the drugs showed similar trends in their variations with energy. For all the penetration depths considered, the buildup factors of the drugs were low in the lower energy region, where the photoelectric effect dominates the mode of interaction. As the energy further increases, the value of buildup factors also increases and attained its highest value at about 0.1 MeV.

At the intermediate energy region, the buildup factors were found to be large. This is due to the contribution of the dominance of the Compton scattering effect. As such, photons were not completely removed but rather stayed longer and caused multiple scattering, which enhanced the buildup factors [12, 15]. At higher energies (E > 1 MeV), the drugs exhibited almost the same value of buildup factors. This implies that in this region, the buildup factors are totally independent of the nature of the drugs. Also, the value of buildup factors for each of the drugs remains almost constant with an increase in energy. This observation is due to the contribution of the pair production effect, which starts to eliminate the effect of Compton scattering. In the region where the buildup factors depend on the nature of the drug, the observable order is BZ > DZ > BP > BA > SB. This implies that the buildup factors followed an inverse course to the μ/ρ and Z_{eff}. Thus, BZ, which has the least value of Z_{eff}, has the maximum value of buildup factors, while SB, which has the highest value of Z_{eff}, has the minimum value. The EBF value of the drugs has a range of 1.08–4.60, 1.16–39.18, 1.20–145.82, 1.30–5679.88, while the EABF has a range of 1.08–4.89, 1.16–46.81, 1.20–190.69, 1.31–7053.72, for 1, 5, 10, and 40 MFPs, respectively.

Figures 7a – 7d and 8a – 8d depict the variation of EBF and EABF of the drugs with penetration depths in the range of 1–40 MFPs at photon energies of 0.015, 0.15, 1.5, and 15 MeV, respectively. Considering the results obtained, it follows

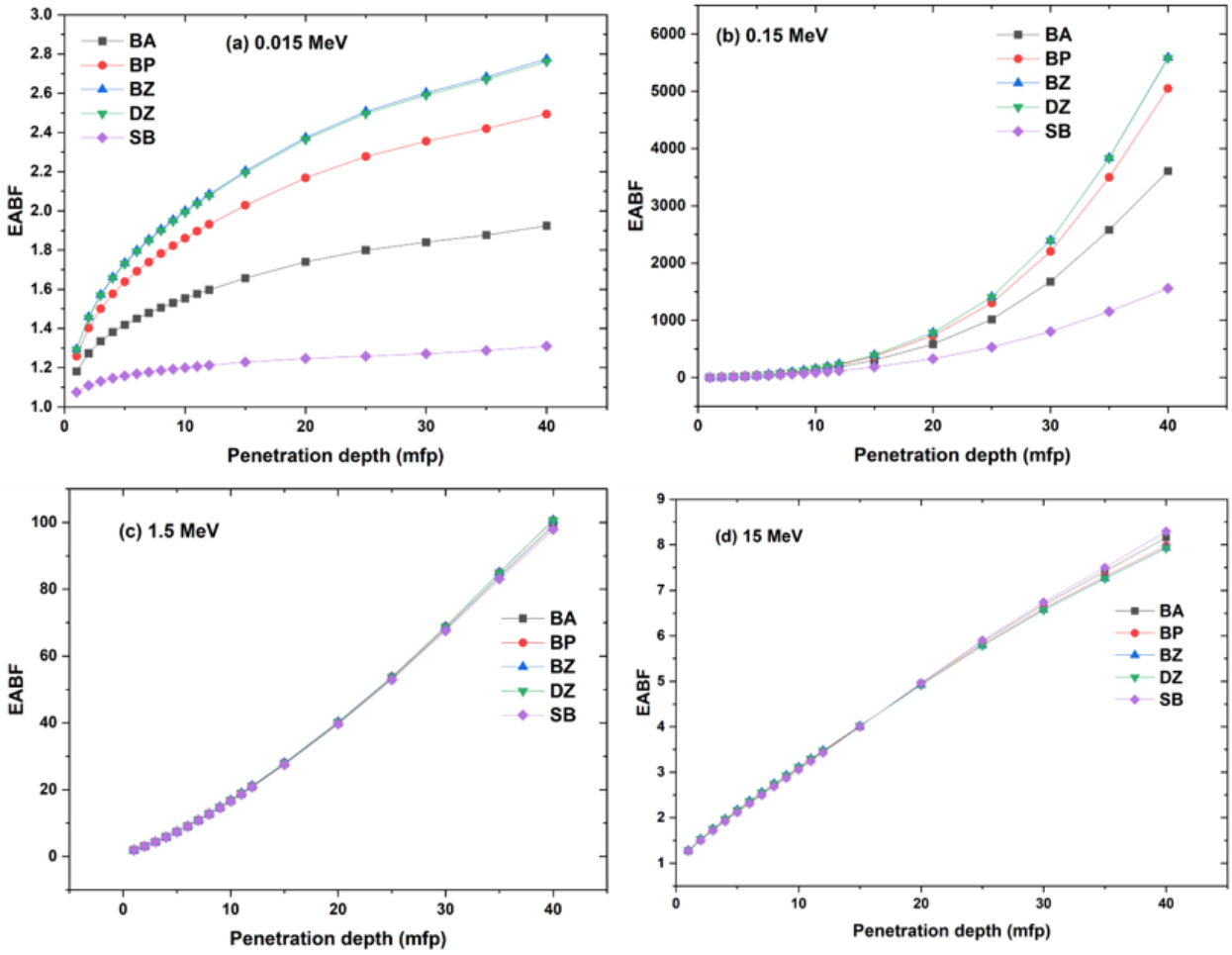

Figure 7. Variation of energy absorption buildup factor of drugs with energy at (a) 1, (b) 5, (c) 10, and (d) 40 MFPs penetration depths for photon interaction.

that the buildup factors increase as the penetration depth increases. However, it was observed that the mode of growth varies across the energy points considered. At 0.015 MeV and 0.15 MeV, buildup factors vary with penetration depth logarithmically (Figures 7a and 8a) and exponentially (Figures 7b and 8b), respectively. At 1.5 and 15 MeV, the variation is approximately a linear curve (Figures 7c, 7d, 8c and 8d). These differences in variation are likely due to the mode of interaction dominating at each of the energy points considered. The results further follow that the buildup factors depend on the chemical composition of the drugs at lower energies (0.015 and 0.15 MeV) (Figures 7a, 7b, 8a and 8b). It is observed that at these lower energies, a smaller value was observed for SB while a larger value was observed for BZ and DZ. For this reason, it follows that the buildup factors increase with a decrease in Z_{eff}. On the contrary, the dependence of buildup factors on the composition of the drugs higher energies, 1.5 and 15 MeV (Figures 7c, 7d, 8c and 8d) is of little or no effect. However, little difference was observed among the drugs for penetration depths in a range of 12–40 MeV. This observable trend is due to the dominance of pair production at this energy [15].

3.4. *Mass stopping power (S(E)/ρ) and mass stopping cross-section (S_c)*

The result of the variation of S(E)/ρ of the investigated drugs with energies in the range of 0.01–400 MeV for proton interactions is shown in Figure 9. In charged particle interactions with matter, S(E)/ρ is an important parameter that is used in determining the range of charged particles in a material [54]. S(E)/ρ is the sum of electronic stopping power and nuclear stopping power. The electronic stopping power, which is based on inelastic collisions with the electrons of a target material, is responsible for the main contributions to the S(E)/ρ. The nuclear stopping power, on the other hand, which is based on elastic collisions with the nucleons of the absorbing medium, is accountable for the least contributions to the S(E)/ρ. However, unlike electronic stopping power, the nuclear stopping power is relevant at low energies [18, 55]. In general, the result obtained (Figure 8) shows that the S(E)/ρ increases as energy increases in the lower energy region (0.01–0.1 MeV), where the contribution of nuclear stopping power is relevant. As such, the S(E)/ρ for all the drugs attained maximum value at approximately 0.1 MeV. On the contrary, at higher energies (E > 0.1 MeV), where the contribution of nuclear stop-

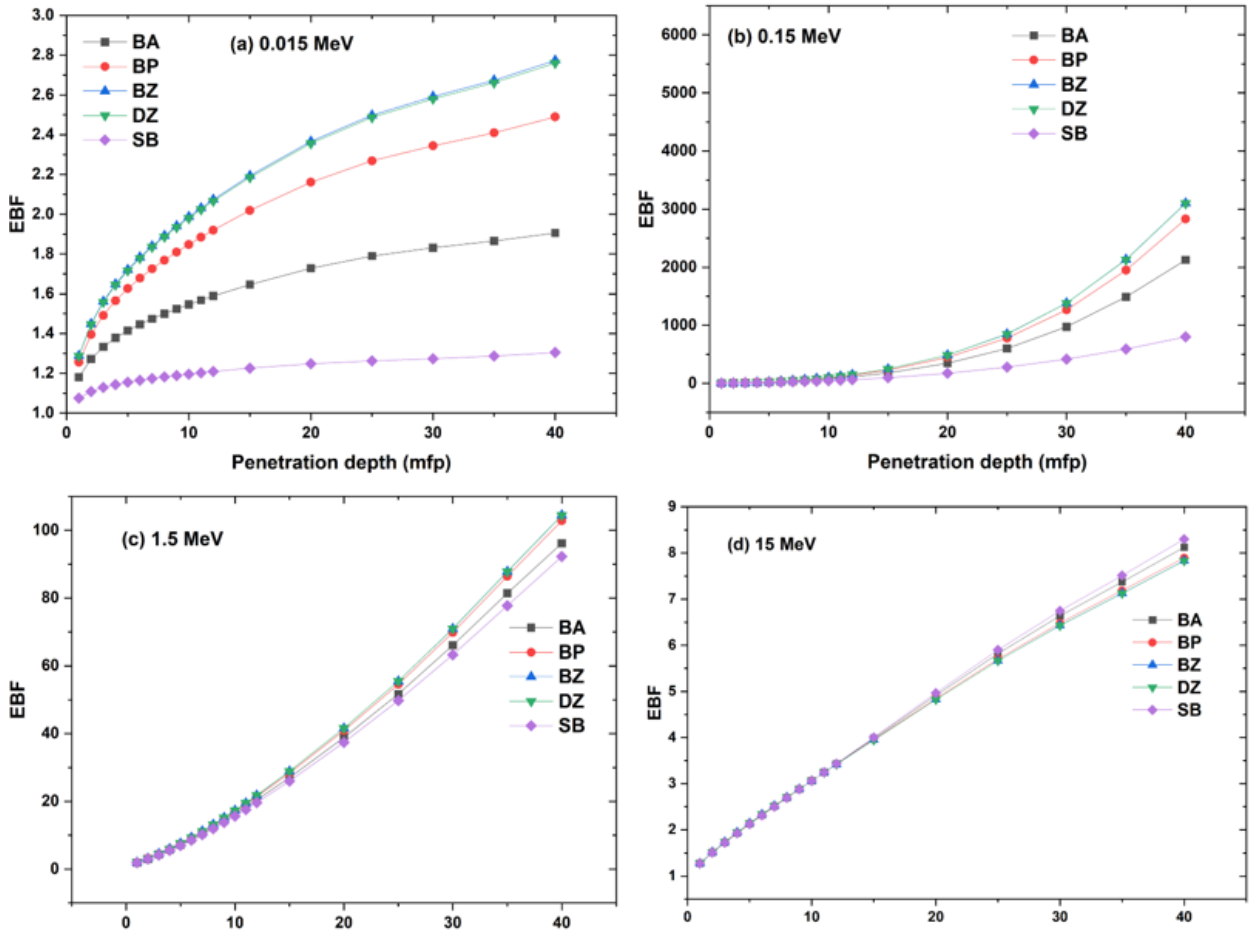

Figure 8. Variation of energy absorption buildup factor of drugs with energy at (a) 1, (b) 5, (c) 10, and (d) 40 MFPs penetration depths for photon interaction.

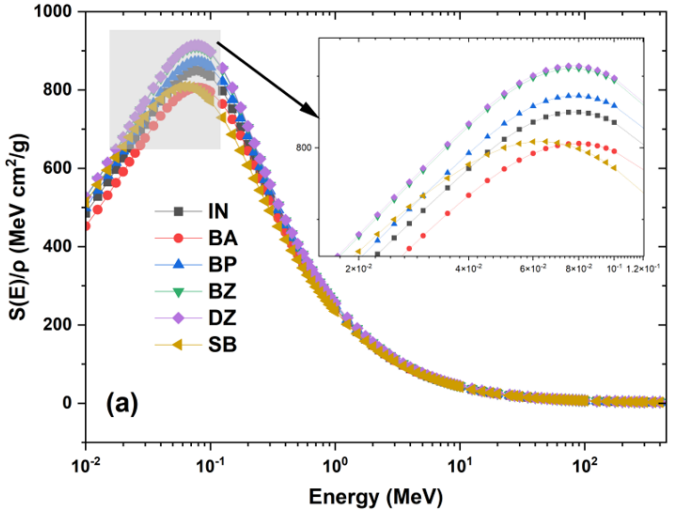

Figure 9. Variation of mass stopping power (S(E)/ρ) of drugs with energy for proton interaction.

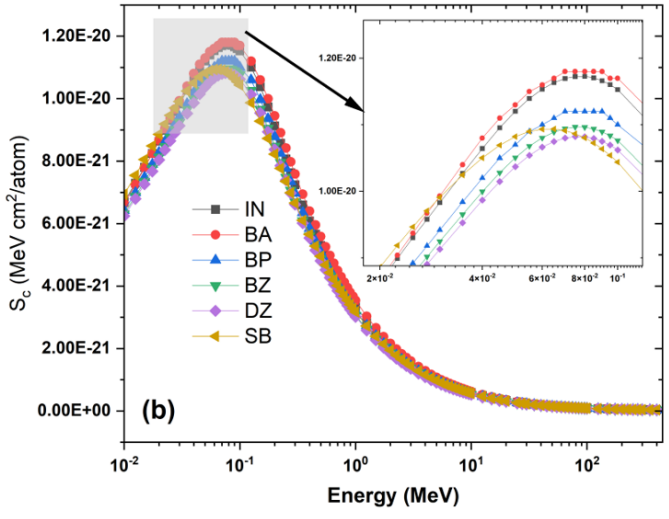

Figure 10. Variation of mass stopping cross-section (S_c) of drugs with energy for proton interaction.

ping power is irrelevant, the S(E)/ρ decreases as the energy increases. This is expected because S(E)/ρ is proportional to $1/\beta^2$, where β represents the ratio of the speed of a charged particle $\left(v = \sqrt{2E/M}\right)$ to the speed of light [18]. Therefore, as the energy (E) of the proton increases, its speed increases and, by

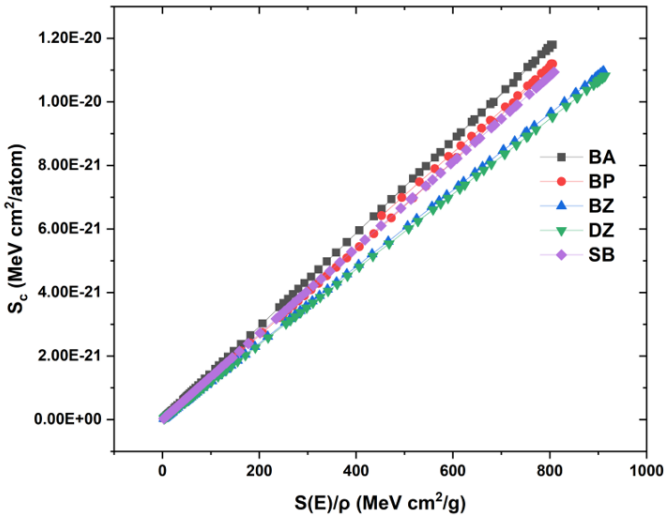

Figure 11. Variation mass stopping power (S(E)/ρ) of drugs with their respective mass stopping cross-section (Sc) with energy for proton interaction.

extension, causes the S(E)/ρ of the drugs to decrease. Going forward, the S(E)/ρ of the drugs shows observable difference at lower energy region (0.01–0.1 MeV). On the contrary, as the energy increases, the difference becomes less noticeable in the higher energy region (E > 0.1 MeV). Similar results have been reported for ^{177}Lu-ethylenediaminetetramethylene phosphonic (^{177}Lu-EDTMP) and ^{177}Lu-methylene diphosphonate (^{177}Lu-MDP) medications used for some bone cancer [9]. Mostly in the lower energy region where the S(E)/ρ of the drugs shows an observable difference, the lowest value was observed for BA while the maximum value was observed for DZ and BZ.

For medical treatments, protons are accelerated by cyclotrons or synchrotrons to therapeutic energies, which are usually between 70 and 250 MeV. To attain the maximal depth of tumors found in clinical practice, the higher end of this range is necessary [39, 56]. Table 3 presents the values of the S(E)/ρ for each of the selected drugs in the clinical energy range (70–250 MeV). The result obtained at this energy range shows an order of DZ > BZ > BP > BA > SB. According to Table 1, the order of the percentage weight of boron present in these drugs is of the order DZ (2.62%) < BZ (2.81%) < BP (5.17%) < BA (17.48%) < SB (59.04%). This implies that at the common energy range applicable in proton therapy (70–250 MeV), the S(E)/ρ of the drugs decreases as the percentage weight of the boron present in the drug increases. This shows that DZ and SB, will respectively, have the maximum and least enhancement factor for proton therapy in clinical applications for 70 to 250 MeV proton energies.

Figure 10 shows the variation of S_c of the investigated drugs with energies in the range of 0.01–40 MeV for proton interactions. In charged particle interactions, S_c is an important parameter in determining the Z_{eff} of the interacting medium [24]. The results obtained revealed that the variation of S_c of the drugs with energy follows a similar trend like those observed for S(E)/ρ in the same energies considered (0.01–0.1 MeV). This similar trend is justified by the direct relationship that exists between S_c and S(E)/ρ as provided in Eq. (7). The result of this direct relationship is further depicted in Figure 11.

4. Conclusion

The μ/ρ, Z_{eff}, N_{eff}, EBF, EABF, S(E)/ρ, and S_c of boric acid (BA), boronophenylalanine (BP), bortezomib (BZ), delanzomib (DZ), and sodium borocaptate (SB) have been investigated in this study. At the lower energy region, the order observed for the μ/ρ among the drugs is SB > BA > BP > DZ > BZ. At the higher energy region, there was no observable difference recorded among the drugs. For photon interaction, at lower energy (E ≤ 0.1 MeV), intermediate energy (0.1 ≤ E ≤ 1 MeV) and higher energy (E ≥ 1 MeV) regions the Z_{eff} of the drugs decreases, remain almost constant, and slightly increases with increase in energy, respectively. For the proton interaction, maximum and minimum value of Z_{eff} were observed for BA and DZ, respectively among the drugs. From the variation of the N_{eff} with Z_{eff}, a direct relationship was observed among the two parameters for both the photon and proton interactions. The buildup factors (EBF and EABF) of the drugs varies with energy and penetration depth. In the region where the buildup factors showed differences among the drugs, the order observed was BZ > DZ > BP > BA > SB. The S(E)/ρ and S_c varies with energy with most of the drugs attaining maximum value at energy of approximately 0.1 MeV. Mostly in the lower energy region where the S(E)/ρ and S_c of the drugs shows an observable difference, the minimum value was observed for BA while the maximum value was observed for DZ and BZ. Finally, from the variation of S_c with the S(E)/ρ, a direct relationship was observed between the two parameters. It is expected that the data obtained from this study will be helpful in fields like chemoradiotherapy and radiation dosimetry.

Data availability

No additional research data were used beyond the content presented in the submitted manuscript.

References

[1] M. Salawu, J. Gbolahan & A. Alabi, "Assessment of radiation shielding properties of polymer-lead (II) oxide composites", Journal of the Nigerian Society of Physical Sciences **3** (2021) 423. https://doi.org/10.46481/jnsps.2021.249

[2] A. Anasthesia, U. Ibrahim, S. Yusuf, D. Joseph, N. Flavious, M. Sidi, S. Shem, A. Mundi, A. Dare & D. Joseph, "Diagnostic reference levels (DRLs) and image quality evaluation for digital mammography in a Nigerian facility", Journal of the Nigerian Society of Physical Sciences **4** (2022) 281. https://doi.org/10.46481/jnsps.2022.734

[3] I. Thierry-Chef, E. Cardis, J. Damilakis, G. Frija, M. Hierath & C. Hoeschen, "Medical applications of ionizing radiation and radiation protection for European patients, population and environment", EPJ Nuclear Science & Technology **8** (2022) 44. https://doi.org/10.1051/epjn/2022044

[4] G. F. Soko, A. B. Burambo, M. M. Mngoya & B. A. Abdul, "Public awareness and perceptions of radiotherapy and their influence on the use of radiotherapy in Dar es Salaam, Tanzania", Journal of Global Oncology **5** (2019) 1. https://doi.org/10.1200/JGO.19.00175

[5] M. Abdel-Wahab, S. S. Gondhowiardjo, A. A. Rosa, Y. Lievens, N. El-Haj, J. A. Polo Rubio, G. B. Prajogi, H. Helgadottir, E. Zubizarreta & A. Meghzifene, "Global radiotherapy: Current status and future directions—white paper", JCO Global Oncology **7** (2021) 827. https://doi.org/10.1200/GO.21.00029.

[6] J.-s. Wang, H.-j. Wang & H.-l. Qian, "Biological effects of radiation on cancer cells", Military Medical Research **5** (2018) 1. https://doi.org/10.1186/s40779-018-0167-4.

[7] N. Behranvand, F. Nasri, R. Zolfaghari Emameh, P. Khani, A. Hosseini, J. Garssen & R. Falak, "Chemotherapy: a double-edged sword in cancer treatment", Cancer Immunology, Immunotherapy **71** (2022) 507. https://doi.org/10.1007/s00262-021-03013-3.

[8] M. Büyüky–ld–z & M. Türemiş, "Radiological properties of some chemotherapy drugs for electron, proton and carbon ion interactions in the energy region 10 keV–400 MeV", Celal Bayar University Journal of Science **19** (2023) 143. https://doi.org/10.18466/cbayarfbe.1140327.

[9] A. Mostafa, M. Uosif, S. A. Issa, M. Zhukovsky, Z. Alrowaili & H. M. Zakaly, "Evaluation of photon, proton, and alpha interaction parameters of EDTMPLu and MDPLu medications used for some bone cancer", Radiation Physics and Chemistry **216** (2024) 111419. https://doi.org/10.1016/j.radphyschem.2023.111419.

[10] T. Tuğrul, "Investigation of mass attenuation coefficients, effective atomic numbers, and effective electron density for some molecules: study on chemotherapy drugs", Journal of Radiation Research and Applied Sciences **13** (2020) 758. https://doi.org/10.1080/16878507.2020.1838040.

[11] B. Aygün & A. Karabulut, "The interaction of neutron and gamma radiation with some cancer drug effect ingredients", Eastern Anatolian Journal of Science **6** (2020) 35. https://dergipark.org.tr/en/pub/eajs/issue/58365/788403.

[12] E. Kavaz, N. Ahmadishadbad & Y. Özdemir, "Photon buildup factors of some chemotherapy drugs", Biomed. Pharmacother. **69** (2015) 34. https://doi.org/10.1016/j.biopha.2014.10.031.

[13] I. Çağlar & G. B. Cengiz, "Evaluation of radiation attenuation properties of some cancer drugs", Ad–yaman University Journal of Science **11** (2021) 503. https://doi.org/10.37094/adyujsci.979888.

[14] F. Akman & M. R. Kaçal, "Investigation of radiation attenuation parameters of some drugs used in chemotherapy in wide energy region", Journal of Radiology and Oncology **2** (2018) 047. https://doi.org/10.29328/journal.jro.1001021.

[15] N. Y. Yorgun & E. Kavaz, "Gamma photon protection properties of some cancer drugs for medical applications", Results in Physics **13** (2019) 102150. https://doi.org/10.1016/j.rinp.2019.02.086.

[16] G. S. Kanberoglu, B. Oto & S. E. Gulebaglan, "Gamma shielding properties of Tamoxifen drug", AIP Conference Proceedings **1815** (2017) 010007. https://doi.org/10.1063/1.4976496.

[17] I. Çağlar, "A review on the gamma ray attenuation behaviours of some chemotherapy drugs used in cancer treatment", in Research on environmental radioactivity, G. B. Cengiz (Ed.), Livre de Lyon, Lyon, France, 2023, pp. 79–91. https://doi.org/10.5281/zenodo.10442949.

[18] A. M. Olaosun & D. E. Shian, "Comprehensive radiological parameterizations of proton and alpha particle interactions for some selected biomolecules: theoretical computation", Radiation. Effects and Defects in Solids **178** (2023) 1109. https://doi.org/10.1080/10420150.2023.2222329.

[19] A. M. Olaosun & D. O. Olaiya, "Elemental characterization and radiation parameters of malignant and healthy breast tissues", Journal of Trace Elements and Minerals **2** (2022) 100023. https://doi.org/10.1016/j.jtemin.2022.100023.

[20] S. Manohara, S. Hanagodimath & L. Gerward, "Energy absorption buildup factors of human organs and tissues at energies and penetration depths relevant for radiotherapy and diagnostics", Journal of Applied Clinical Medical Physics **12** (2011) 296. https://doi.org/10.1120/jacmp.v12i4.3557.

[21] O. Kadri & A. Alfuraih, "Photon energy absorption and exposure buildup factors for deep penetration in human tissues", Nuclear Science and Techniques **30** (2019) 176. https://doi.org/10.1007/s41365-019-0701-4.

[22] N. A. Alsaif, Y. Elmahroug, B. M. Alotaibi, H. A. Alyousef, N. Rekik, A. W. M. Hussein, R. Chand & U. Farooq, "Calculating photon buildup factors in determining the γ-ray shielding effectiveness of some materials susceptible to be used for the conception of neutrons and γ-ray shielding", Journal of Materials Research and Technology **11** (2021) 769. https://doi.org/10.1016/j.jmrt.2021.01.052.

[23] A. S. Almutairi & K. T. Osman, "Mass stopping power and range of protons in biological human body tissues (ovary, lung and breast)", International Journal of Medical Physics, Clinical Engineering and Radiation Oncology **11** (2021) 48. https://doi.org/10.4236/ijmpcero.2022.111005.

[24] S. Prabhu, S. Jayaram, B. Bubbly & S. Gudennavar, "A simple software for swift computation of photon and charged particle interaction parameters: PAGEX", Applied Radiation and Isotopes **176** (2021) 109903. https://doi.org/10.1016/j.apradiso.2021.109903.

[25] V. Bregadze, I. Sivaev & S. Glazun, "Polyhedral boron compounds as potential diagnostic and therapeutic antitumor agents", Anti-Cancer Agents in Medicinal Chemistry **6** (2006) 75. https://doi.org/10.2174/187152006776119180.

[26] M. K. Gündüz, M. Bolat, G. Kaymak, D. Berikten, D. A. Köse, "Therapeutic effects of newly synthesized boron compounds (BGM and BGD) on hepatocellular carcinoma", Biological Trace Element Research **200** (2022) 134. https://doi.org/10.1007/s12011-021-02647-9.

[27] E. Meiyanto, R. A. Susidarti, R. I. Jenie, R. Y. Utomo, D. Novitasari, F. Wulandari & M. Kirihata, "Synthesis of new boron containing compound (CCB-2) based on curcumin structure and its cytotoxic effect against cancer cells", Journal of Applied Pharmaceutical Science **10** (2020) 060. https://doi.org/10.7324/JAPS.2020.102010.

[28] E. Cebeci, B. Yüksel & F. Şahin, "Anti-cancer effect of boron derivatives on small-cell lung cancer", Journal of Trace Elements in Medicine and Biology **70** (2022) 126923. https://doi.org/10.1016/j.jtemb.2022.126923.

[29] G. J. Kubicek, R. S. Axelrod, M. Machtay, P. H. Ahn, P. R. Anne, S. Fogh, D. Cognetti, T. J. Myers, W. J. Curran Jr & A. P. Dicker, "Phase I trial using the proteasome inhibitor bortezomib and concurrent chemoradiotherapy for head-and-neck malignancies", International Journal of Radiation Oncology, Biology, Physics **83** (2012) 1192. https://doi.org/10.1016/j.ijrobp.2011.09.023.

[30] R. M. Eager, C. C. Cunningham, N. N. Senzer, J. Stephenson, S. P. Anthony, S. J. O'Day, G. Frenette, A. C. Pavlick, B. Jones & M. Uprichard, "Phase II assessment of talabostat and cisplatin in second-line stage IV melanoma", BMC Cancer **9** (2009) 263. https://doi.org/10.1186/1471-2407-9-263.

[31] K. Narra, S. R. Mullins, H.-O. Lee, B. Strzemkowski-Brun, K. Magalong, V. J. Christiansen, P. A. McKee, B. Egleston, S. J. Cohen & L. M. Weiner, "Phase II trial of single agent Val-boroPro (Talabostat) inhibiting Fibroblast Activation Protein in patients with metastatic colorectal cancer", Cancer biology & therapy **6** (2007) 1691. https://doi.org/10.4161/cbt.6.11.4874.

[32] R. Eager, C. Cunningham, N. Senzer, D. Richards, R. Raju, B. Jones, M. Uprichard & J. Nemunaitis, "Phase II trial of talabostat and docetaxel in advanced non-small cell lung cancer", Clinical Oncology **21** (2009) 464. https://doi.org/10.1016/j.clon.2009.04.007.

[33] A. Ç. Gündoğdu, N. S. Ar–, A. Höbel, G. Şenol, Ö. Eldiven & F. Kar, "Boric acid exhibits anticancer properties in human endometrial cancer Ishikawa cells", Cureus **15** (2023) e44277. https://doi.org/10.7759/cureus.44277.

[34] E. Kahraman & E. Göker, "Boric acid exerts anti-cancer effect in poorly differentiated hepatocellular carcinoma cells via inhibition of AKT signaling pathway", Journal of Trace Elements in Medicine and Biology **73** (2022) 127043. https://doi.org/10.1016/j.jtemb.2022.127043.

[35] M. Wang, L. Liang, J. Lu, Y. Yu, Y. Zhao, Z. Shi, H. Li, X. Xu, Y. Yan & Y. Niu, "Delanzomib, a novel proteasome inhibitor, sensitizes breast cancer cells to doxorubicin-induced apoptosis", Thoracic Cancer **10** (2019) 918. https://doi.org/10.1111/1759-7714.13030.

[36] K. Y. Guo, L. Han, X. Li, A. V. Yang, J. Lu, S. Guan, H. Li, Y. Yu, Y. Zhao & J. Yang, "Novel proteasome inhibitor delanzomib sensitizes cervical cancer cells to doxorubicin-induced apoptosis via stabilizing tumor suppressor proteins in the p53 pathway", Oncotarget **8** (2017) 114123. https://doi.org/10.18632/oncotarget.23166.

[37] P. Bláha, C. Feoli, S. Agosteo, M. P. Cammarata, R. Catalano, M. Ciocca, G. A. P. Cirrone, V. Conte & G. Cuttone, "The proton-boron reaction increases the radiobiological effectiveness of clinical low-and high-energy proton beams: novel experimental evidence and perspectives", Frontiers in Oncology **11** (2021) 682647. https://doi.org/10.3389/fonc.2021.682647.

[38] C. Van Waes, A. A. Chang, P. F. Lebowitz, C. H. Druzgal, Z. Chen, Y. A. Elsayed, J. B. Sunwoo, S. F. Rudy, J. C. Morris & J. B. Mitchell,

"Inhibition of nuclear factor-κB and target genes during combined therapy with proteasome inhibitor bortezomib and reirradiation in patients with recurrent head-and-neck squamous cell carcinoma", International Journal of Radiation Oncology, Biology, Physics **63** (2005) 1400. https://doi.org/10.1016/j.ijrobp.2005.05.007.

[39] R. Mohan & D. Grosshans, "Proton therapy–present and future", Advanced Drug Delivery Reviews **109** (2017) 26. https://doi.org/10.1016/j.addr.2016.11.006.

[40] J. M. Ryckman, V. Ganesan, A. Kusi Appiah, C. Zhang & V. Verma, "National practice patterns of proton versus photon therapy in the treatment of adult patients with primary brain tumors in the United States", Acta Oncologica. **58** (2019) 66. https://doi.org/10.1080/0284186X.2018.1512755.

[41] Z. Chen, M. M. Dominello, M. C. Joiner & J. W. Burmeister, "Proton versus photon radiation therapy: A clinical review", Frontiers in Oncology **13** (2023) 1133909. https://doi.org/10.3389/fonc.2023.1133909.

[42] N. H. Tran, T. Shtam, Y. Y. Marchenko, A. L. Konevega & D. Lebedev, "Current state and prospectives for proton boron capture therapy", Biomedicines **11** (2023) 1727. https://doi.org/10.3390/biomedicines11061727.

[43] G. Cirrone, L. Manti, D. Margarone, G. Petringa, L. Giuffrida, A. Minopoli, A. Picciotto, G. Russo, F. Cammarata & P. Pisciotta, "First experimental proof of Proton Boron Capture Therapy (PBCT) to enhance protontherapy effectiveness," Scientific Reports **8** (2018) 1141. https://doi.org/10.1038/s41598-018-19258-5.

[44] I. N. Zavestovskaya, A. L. Popov, D. D. Kolmanovich, G. V. Tikhonowski, A. I. Pastukhov, M. S. Savinov, P. V. Shakhov, J. S. Babkova, A. A. Popov & I. V. Zelepukin, "Boron nanoparticle-enhanced proton therapy for cancer treatment", Nanomaterials **13** (2023) 2167. https://doi.org/10.3390/nano13152167.

[45] L. Gerward, N. Guilbert, K. B. Jensen & H. Levring, "WinXCom—a program for calculating X-ray attenuation coefficients", Radiation Physics and Chemistry **71** (2004) 653. https://doi.org/10.1016/j.radphyschem.2004.04.040.

[46] M. Berger, ESTAR, PSTAR, ASTAR. A PC Package for Calculating Stopping Powers and Ranges of Electrons, Protons and Helium Ions, Version 2 (International Atomic Energy Agency, Vienna, 1993). https://inis.iaea.org/records/pf2sy-yag85.

[47] U. Akbaba, E. Şakar, M. Sayyed, B. Alim & Ö. F. Özpolat, "Evaluation of photon interaction parameters of Anti-HIV drugs", Radiation Physics and Chemistry **201** (2022) 110441. https://doi.org/10.1016/j.radphyschem.2022.110441.

[48] R. Hill, B. Healy, L. Holloway, Z. Kuncic, D. Thwaites & C. Baldock, "Advances in kilovoltage x-ray beam dosimetry", Physics in Medicine & Biology **59** (2014) R183. https://doi.org/10.1088/0031-9155/59/6/R183.

[49] E. B. Podgorsak, "Treatment Machines for External Beam Radiotherapy", in Radiation Oncology Physics: A Handbook for Teachers and Students, E. B. Podgorsak (Ed.), International Atomic Energy Agency, Vienna, Austria, 2005, pp. 123–160. https://www.osti.gov/etdeweb/biblio/20628272.

[50] E. K. Hansen & M. Roach, Handbook of Evidence-Based Radiation Oncology, Springer, Cham, Switzerland, 2018, pp. 1–969. https://doi.org/10.1007/978-3-319-62642-0.

[51] K. A. Camphausen and R. C. Lawrence, "Principles of radiation therapy", in Cancer management: a multidisciplinary approach, R. Pazdur, L. R. Coia, W. J. Hoskins, & L. D. Wagman (Eds.), CMP Medica, New York, USA, 2008, pp. 221–230. IOS Press, Amsterdam and Springer, Dordrecht, Netherlands, 2008, pp. 221–230. https://thymic.org/wp-content/uploads/2021/05/Radiation-Principles.pdf.

[52] Y. Lemoigne and A. Caner, Radiotherapy and Brachytherapy, IOS Press, Amsterdam and Springer, Dordrecht, Netherlands, 2009, pp. 1–239. https://doi.org/10.1007/978-90-481-3097-9.

[53] M. Kurudirek & T. Onaran, "Calculation of effective atomic number and electron density of essential biomolecules for electron, proton, alpha particle and multi-energetic photon interactions", Radiation Physics and Chemistry **112** (2015) 125. https://doi.org/10.1016/j.radphyschem.2015.03.034.

[54] A. Bozkurt, "Monte Carlo calculation of proton stopping power and ranges in water for therapeutic energies", EPJ Web of Conferences, **154** (2017) 01007. https://doi.org/10.1051/epjconf/201715401007.

[55] M. Usta & M. Ç. Tufan, "Stopping power and range calculations in human tissues by using the Hartree-Fock-Roothaan wave functions", Radiation Physics and Chemistry **140** (2017) 43. https://doi.org/10.1016/j.radphyschem.2017.03.005.

[56] R. Mohan, "A review of proton therapy–Current status and future directions", Precision Radiation Oncology **6** (2022) 164. https://doi.org/10.1002/pro6.1149.